Robust finite-temperature disordered Mott-insulating phases in inhomogeneous Fermi-Fermi mixtures with density and mass imbalance

Anzi Hu,[1,2] M. M. Maśka,[3] Charles W. Clark,[1] and J. K. Freericks[4]

[1]*Joint Quantum Institute, University of Maryland and National Institute of Standard and Technology, Gaithersburg, Maryland 20899, USA*

[2]*Department of Physics, American University, Washington, DC 20016, USA*

[3]*Department of Theoretical Physics, Institute of Physics, University of Silesia, PL-40007 Katowice, Poland*

[4]*Department of Physics, Georgetown University, Washington, DC 20057, USA*

(Received 20 April 2015; published 22 June 2015)

Ultracold mixtures of different atomic species have great promise for realizing novel many-body phenomena. In a binary mixture of fermions with a large mass difference and repulsive interspecies interactions, a disordered Mott-insulator phase can occur. This phase displays an incompressible total density, although the relative density remains compressible. We use strong-coupling and Monte Carlo calculations to show that this phase exists for a broad parameter region for ultracold gases confined in a harmonic trap on a three-dimensional optical lattice, for experimentally accessible values of the trap parameters.

DOI: 10.1103/PhysRevA.91.063624 PACS number(s): 67.85.−d, 03.75.−b, 05.30.Fk, 71.10.Fd

I. INTRODUCTION

The advancement of ultracold-atom experiments with both homonuclear fermionic mixtures [1–6] and heteronuclear fermionic mixtures [7–9] demonstrates the possibility of realizing a quantum degenerate binary fermionic mixture with great mass and/or density imbalance. Previous theoretical studies have focused on ground-state or low-temperature phases of the repulsive imbalanced fermion mixtures, including discussions of the segregated phase or itinerant ferromagnetism in density imbalanced systems [4,10–17] and the crystallization and complex long-range density ordering in mass imbalanced systems [11,18–23]. These complex phases are often unstable to thermal fluctuations and the inhomogeneity of the trapping potential and they have yet to be realized in experiments because the ordering temperature is too low. Broadly speaking, many-body phases of atomic mixtures of bosonic and fermionic species in optical lattices have attracted a wide range of research interests and have been shown to display extremely rich many-body ordering, such as the appearance of the supersolid [24–29], the Fulde-Ferrell and Larkin-Ovchinnikov phases (see Ref. [30] for a review), and the paired and counterflow superfluid for both Bose [31–35] and Bose-Fermi mixtures [36]. These studies are either focused on the ground state or extremely low temperature. These phases require, to various degree, the existence of phase coherence of the superfluid state and are generally susceptible to large thermal fluctuations and hence only exist at extremely low temperatures.

It is of great importance to explore new many-body phenomena that are robust against thermal fluctuations and inhomogeneity. Here we show an example of such a robust many-body phase: a disordered Mott-insulator (DMI) phase in a mixture of localized and itinerant fermions. The DMI phase corresponds to a situation where the density of each species of fermions can vary, as long as the total density is fixed at exactly one. If we ignore any possible ordered density wave phases, or phase separation, then this phase would appear as a zero-temperature phase transition in the ground state as the interspecies interaction is increased beyond the Mott transition, just like in the Fermi or Bose-Hubbard models. At finite temperature, the phase only approximately exists because the compressibility to the total density becomes finite [23,37]. Hence, at finite temperature, we always refer to the system as having a smooth crossover to the DMI phase. Of course, for most fillings of the fermions (with the total still equal to one), the system will undergo phase separation to the segregated phase as the temperature is lowered [11], precluding the direct observation of the quantum phase transition for the DMI.

We show that in an inhomogeneous system, the DMI phase exhibits an incompressible total density while the relative density is compressible. The DMI also exists in cases of large number imbalance and asymmetries in the trapping potentials for the two fermionic species. It can be detected with procedures similar to those used for detecting a Mott-insulator phase of fermionic ^{40}K in Refs. [1,38]. The DMI phases we discussed here can also exist in the Fermi-Bose mixtures, which have been realized in experiments with ^{87}Rb-^{40}K mixtures [39–41], which focus on how the impurity of fermions changes the bosonic superfluid–Mott-insulator transition, and in ^{170}Yb-^{173}Yb mixtures, where the interaction and filling induced phases in a strongly correlated Bose-Fermi system with both repulsive and attractive inter-species interactions are studied [42]. In the regime of a strongly repulsive interspecies interaction, a dual Mott insulator occurs where the total density of bosons and fermions are incompressible, while the individual density is compressible [42]. This phase is similar to the DMI phase, although the theoretical study in [42] neglected the coherent hopping of both fermions and bosons.

It is also worth noting that for many relative densities of the particles, the system will be susceptible to segregation, which is usually a first-order phase transition, but occurs at temperatures too low to be seen with current experimental technology. But the behavior of the system in the DMI region is distinctive, with interesting properties which are unlike that of a noninteracting mixture.

We treat a mixture of N_f heavy and N_c light fermions in a cubic lattice with lattice constant a and additional isotropic harmonic potentials, at finite temperature $T > 0$. Due to the mass asymmetry, $M_f > M_c$, there is a large difference in the

hopping energies of the two species. In this work, it is a hopping imbalance, not a mass difference, that is most critical. A mass imbalance is the easiest way to achieve a hopping imbalance. Thus, the system can be effectively described by a model of localized and itinerant fermions [11,43]. Its Hamiltonian is written as

$$H = -J\sum_{\langle j,j'\rangle} c_j^\dagger c_{j'} + U\sum_j c_j^\dagger c_j f_j^\dagger f_j + \sum_j [(V_{c,j}-\mu_c)c_j^\dagger c_j + (V_{f,j}-\mu_f)f_j^\dagger f_j], \quad (1)$$

where c_j and f_j are the annihilation operators for light and heavy fermions at lattice site j, J is the hopping energy for the light fermions, $U > 0$ is the repulsive interaction between light and heavy fermions, $\mu_{c\text{ or }f}$ is the chemical potential for light or heavy fermions and $V_{c\text{ or }f,j}$ is the corresponding harmonic trapping potential at lattice site j, specifically $V_{c\text{ or }f,j} = (M_{c\text{ or }f}/2)\omega_{c\text{ or }f}^2 r_j^2$ where $\omega_{c\text{ or }f}$ is the trapping frequency for heavy or light fermions and r_j is the distance of the lattice site j from the center of the trap. It is convenient to define $L_{c\text{ or }f}$ through $V_{c\text{ or }f,j} = J(r_j/L_{c\text{ or }f})^2$. The total particle number of each species, $N_{c\text{ or }f}$, is determined by the chemical potentials $\mu_{c\text{ or }f}$.

Although we assume that the heavy species' hopping is zero, results given here should directly carry through for small nonzero hopping, especially in achieving a thermalization of the heavy species [44]. One might wonder how a system with vanishing hopping can sample all possible heavy configurations in a thermodynamic sense, when there is no direct movement of the heavy particles in the Hamiltonian. This issue already arose in the study of the Ising model, which has no spin-flip terms in the Hamiltonian, yet averages over all possible spin configurations having a transition from a paramagnetic phase to an ordered phase. The Falicov-Kimball model is dealt with in exactly the same way. From run to run, we expect the experiment to be sampling the system with a heavy-atom configuration that is from a high-probability state in the thermodynamic average of possible states. This can easily occur during the ramping up of the lattice if the system maintains thermodynamic equilibrium due to an adiabatic ramp. Then the system will pick the appropriate heavy-atom configuration by moving the heavy atoms to the right locations while the heavy hopping is small but not yet so small that we can neglect it. The sampling of the experiment will then be similar to a Monte Carlo sampling over configurations after the algorithm has thermalized. If the hopping is large enough that there remains some heavy-atom motion during the experiment, the heavy atoms should only move between high-probability configurations, which will continue to maintain the behavior needed for an experimental realization.

We use both the Monte Carlo (MC) calculations and the strong-coupling (SC) method [35] to investigate the finite-temperature phases of these mixtures. The MC calculations are based on a modified Metropolis algorithm, developed for interacting systems with both quantum and classical degrees of freedom. For a given configuration of heavy fermions, the Hamiltonian is a one-particle Hamiltonian representing itinerant free fermions in a nonuniform potential defined by the positions of the heavy fermions. As such, it can be easily numerically diagonalized, giving states of the light fermions and their energy spectrum. In each MC step, the configuration of the heavy fermions is modified, the Hamiltonian is then diagonalized, and the resulting configuration is accepted or rejected according to the Metropolis criterion. In this criterion, however, the free energy of the fermionic subsystem is used instead of the internal energy. This method has been successfully applied to the Falicov-Kimball model and its details are given in Ref. [45]. The SC formalism is discussed in Sec. II. In Sec. III, we discuss interesting features of the disordered MI phase based on the SC and MC calculations and we show that the SC derivations and the MC calculations are in excellent agreement for the parameter region considered in this article. The summary and future directions are in Sec. IV.

II. STRONG-COUPLING EXPANSION FORMALISM

We summarize the main results of our derivation. A more detailed discussion of the derivation can be found in [35]. To simplify the notation, we introduce $\bar{\mu}_{c,j}(n_{f,j})$ and $\bar{\mu}_{f,j}(n_{f,j})$ for the light and heavy fermions in the atomic limit at site j,

$$\bar{\mu}_{c,j}(n_{f,j}) \equiv \mu_c - V_{c,j} - Un_{f,j} \quad (2)$$

and

$$\bar{\mu}_{f,j}(n_{f,j}) \equiv (\mu_f - V_{f,j})n_{f,j}. \quad (3)$$

Here $n_{f,j} = 0,1$ denotes whether there is a heavy particle at site j. The effective fugacities are written as

$$\phi_{c,j}(n_{f,j}) = \exp[\beta\bar{\mu}_{c,j}(n_{f,j})] \quad (4)$$

and

$$\phi_{f,j}(n_{f,j}) = \exp[\beta\bar{\mu}_{f,j}(n_{f,j})]. \quad (5)$$

After the second-order expansion of the time-evolution operator of the hopping term, the partition function has two parts: the atomic-limit partition function $\mathcal{Z}^{(0)}$ and the second-order expansion term $\mathcal{Z}^{(2)}$ as

$$\mathcal{Z} = \mathcal{Z}^{(0)}(1+\mathcal{Z}^{(2)}), \quad (6)$$

where

$$\mathcal{Z}^{(0)} = \Pi_j \mathcal{Z}_j^{(0)} = \Pi_j \left\{\sum_{n_{f,j}} \phi_{f,j}[1+\phi_{c,j}]\right\} \quad (7)$$

and

$$\mathcal{Z}^{(2)} = \frac{\beta}{2}\sum_{j,k} J^2 \sum_{n_{f,j}n_{f,k}} \frac{\phi_{f,j}\phi_{f,k}}{\mathcal{Z}_j^{(0)}\mathcal{Z}_k^{(0)}} \frac{\phi_{c,j}-\phi_{c,k}}{\bar{\mu}_{c,j}-\bar{\mu}_{c,k}}. \quad (8)$$

The density and the entropy of light and heavy fermions at site j can be derived from the partition function. The density for the light particles is written as

$$\rho_{c,j} = \rho_{c,j}^{(0)} + \rho_{c,j}^{(2)}, \quad (9)$$

where

$$\rho_{c,j}^{(0)} = \frac{\sum_{n_{f,j}} \phi_{c,j}\phi_{f,j}}{\mathcal{Z}_j^{(0)}} \quad (10)$$

and

$$\rho^{(2)}_{c,j} = \sum_k J^2 \sum_{n_{f,j} n_{f,k}} \frac{\phi_{b,j}\phi_{b,k}}{\mathcal{Z}^{(0)}_j \mathcal{Z}^{(0)}_k} \Bigg[\beta \frac{(1-\rho^{(0)}_{c,j})\phi_{c,j} + \rho^{(0)}_{c,j}\phi_{c,k}}{\bar{\mu}_{c,j} - \bar{\mu}_{c,k}} + \frac{\phi_{c,k} - \phi_{c,j}}{[\bar{\mu}_{c,j} - \bar{\mu}_{c,k}]^2} \Bigg]. \tag{11}$$

The density for the heavy particles is

$$\rho_{f,j} = \rho^{(0)}_{f,j} + \rho^{(2)}_{f,j}, \tag{12}$$

where

$$\rho^{(0)}_{f,j} = \frac{\sum_{n_{f,j}} n_{f,j}(\phi_{c,j}+1)\phi_{f,j}}{\mathcal{Z}^{(0)}_j} \tag{13}$$

and

$$\rho^{(2)}_{f,j} = \sum_k J^2 \sum_{n_{f,j} n_{f,k}} \beta\big(n_{f,j} - \rho^{(0)}_{f,j}\big) \frac{\phi_{b,j}\phi_{b,k}}{\mathcal{Z}^{(0)}_j \mathcal{Z}^{(0)}_k} \frac{\phi_{c,j} - \phi_{c,k}}{\bar{\mu}_{c,j} - \bar{\mu}_{c,k}}. \tag{14}$$

The local entropy at site j also contains two parts: the entropy at the site j in the atomic limit,

$$S^{(0)}_j / k_B = \ln\big(\mathcal{Z}^{(0)}_j\big) - \beta\epsilon_j, \tag{15}$$

where ϵ_j corresponds to the on-site energy at site j in the atomic limit,

$$\epsilon_j = \frac{1}{\mathcal{Z}^{(0)}_j} \sum_{n_{f,j}} [\bar{\mu}_{f,j}\phi_{f,j}(1+\phi_{c,j}) + \bar{\mu}_{c,j}\phi_{f,j}\phi_{c,j}], \tag{16}$$

and the averaged contributions from the hopping at site j,

$$S^{(2)}_j / k_B = -\frac{\beta^2}{2} \sum_k J^2 \sum_{n_{f,j} n_{f,k}} \frac{\phi_{f,j}\phi_{f,k}}{\mathcal{Z}^{(0)}_j} \mathcal{Z}^{(0)}_k [\bar{\mu}_{c,j} - \bar{\mu}_{c,k}] \times \{[\phi_{c,j} - \phi_{c,k}][\bar{\mu}_{f,j} + \bar{\mu}_{f,k} - \epsilon_j - \epsilon_k] + \bar{\mu}_{c,j}\phi_{c,j} - \bar{\mu}_{c,k}\phi_{c,k}\}. \tag{17}$$

The double occupancy d_j is determined as the joint probability of having exactly one heavy and one light particle at site j. It is derived from the density expressions as follows:

$$d_j = d^{(0)}_j + d^{(2)}_j, \tag{18}$$

where

$$d^{(0)}_j = \frac{\phi_{b,j}\phi_{c,j}|_{n_{f,j}=1}}{\mathcal{Z}^{(0)}_j} \tag{19}$$

and

$$d^{(2)}_j = \sum_k J^2 \sum_{n_{f,j} n_{f,k}} \frac{\phi_{f,j}\phi_{f,k}}{\mathcal{Z}^{(0)}_j \mathcal{Z}^{(0)}_k} \Bigg\{ -\beta d^{(0)}_j \frac{\phi_{c,j} - \phi_{c,k}}{\bar{\mu}_{c,j} - \bar{\mu}_{c,k}} + \delta_{n_{f,j},1} \Bigg[\beta \frac{\phi_{c,j}}{\bar{\mu}_{c,j} - \bar{\mu}_{c,k}} + \frac{\phi_{c,k} - \phi_{c,j}}{(\bar{\mu}_{c,j} - \bar{\mu}_{c,k})^2} \Bigg] \Bigg\}. \tag{20}$$

The average double occupancy is determined as $D = N^{-1}\sum_j d_j$, where N is the lesser of the total particle numbers for the light and heavy particles.

III. RESULTS

A. Main features

An intrinsic feature of ultracold-atom experiments is the spatial inhomogeneity induced by the existence of a trapping potential. With the MC calculation, we simulate experimental *in situ* images of atoms in trapped systems through snapshots generated by the MC simulation (after thermalization) [11]. These snapshots show a striking feature of the DMI. Figures 1 and 2 show a series of possible experimental realizations of the DMI phases for three particular choices of N_f/N_c. The snapshots of the density distribution are generated by a MC simulation for a two-dimensional lattice in a harmonic trap. We consider the process of adding heavy fermions as impurities into an ultracold gas of light fermions, with a strong repulsive

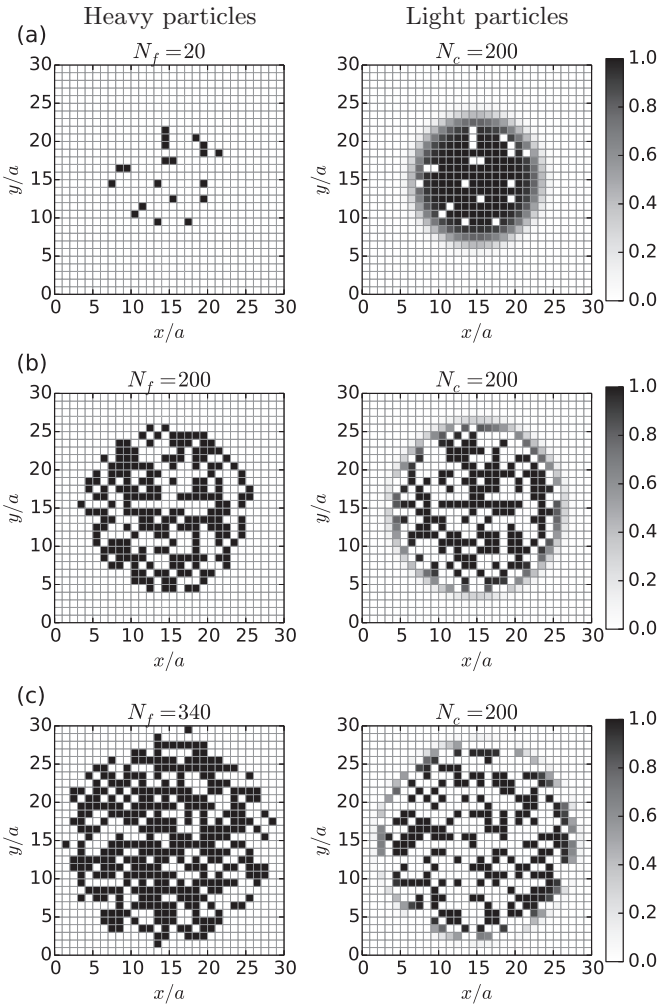

FIG. 1. Monte Carlo snapshots of the disordered MI phase in a trapped two-dimensional lattice system of light and heavy mixtures. The light particle number (right column) is fixed at 200 and the heavy particle numbers (left column) are (a) 20, (b) 200, and (c) 340. The interaction U is $50J$, the trap frequencies are set by $L_c = L_f = 2a$, and the temperature is $2J/k_B$. The density distribution of the light and heavy particles appears disordered but the sum of them, i.e., the total density, remains at unit filling near the center for all of the cases. This plateau of the total density in the center of the trap remains in the MI phase.

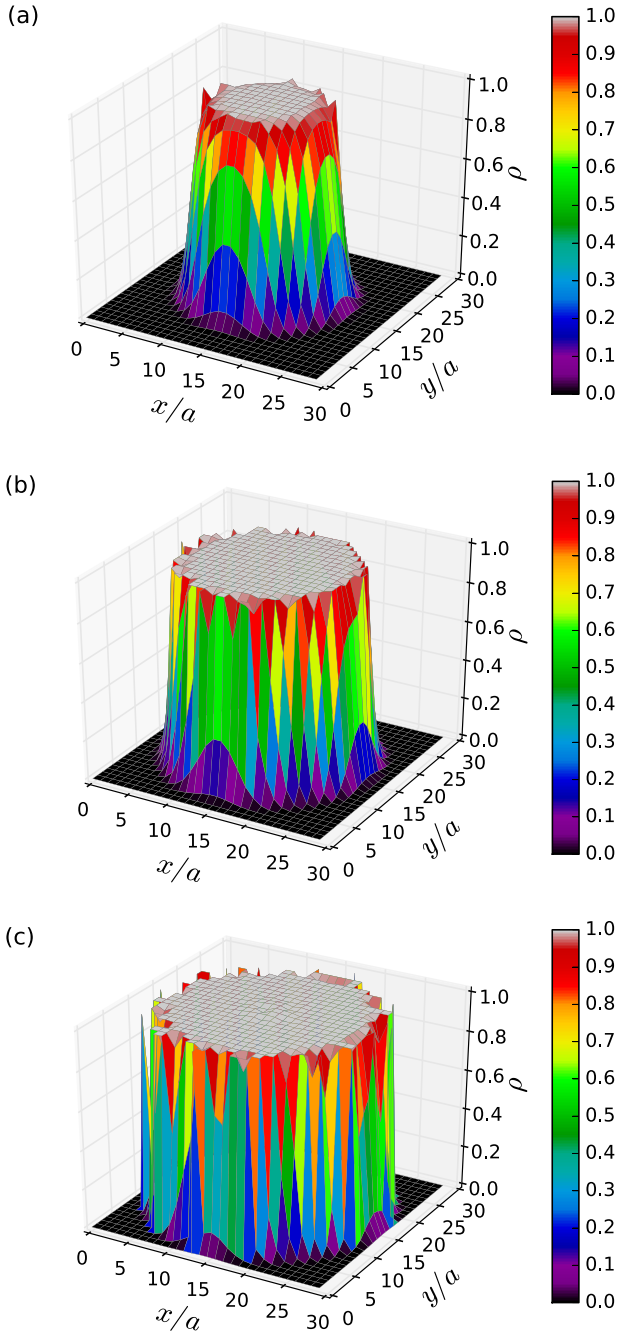

FIG. 2. (Color online) Spatial distribution of the total density in the cases presented in Fig. 1. The number of light fermions is 200; the number of heavy fermions is (a) 20, (b) 200, and (c) 340.

interaction between the light and heavy fermions. If no heavy fermions are present, the light fermions form a band insulator at the center of the trap as a result of the trapping potential. When heavy fermions are added, one heavy fermion leads to the modification of the total wave function of the light fermions. In the three panels shown in Fig. 1, the individual density distribution is disordered. But when we compare the distributions of the two atomic species, they are perfectly complimentary. Around the center of the trap, the total density *always* remains at unit filling, as shown in Fig. 2. The radius of the MI plateau in the total density increases as more heavy

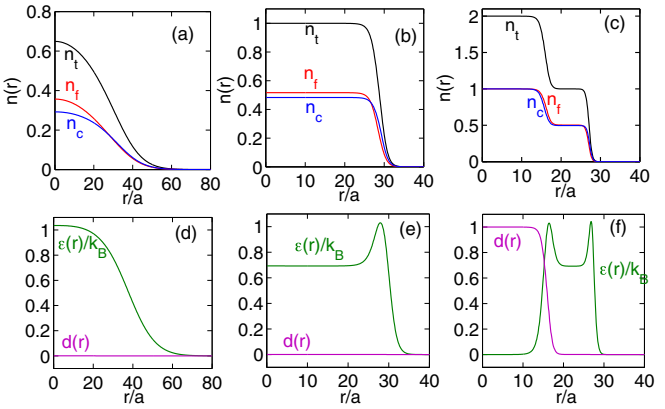

FIG. 3. (Color online) Radial distribution of densities, entropy, and double occupancy for different trapping frequencies in a three-dimensional (3D) system. The interaction is fixed at $U = 50J$ and temperature at $T = 2J/k_B$. There are 5×10^4 heavy and light fermions. The trapping frequencies are the same for both heavy and light fermions, $L_c = L_f = L$. (a)–(c) Radial distribution of the total density n_t (black line), heavy fermions n_f (red line), and light fermions n_c (blue line). (d)–(f) Radial distribution of the entropy $\epsilon(r)$ (green line) and the double occupancy $d(r)$ (magenta line). (a),(d) The trapping frequency is set by $L = 16.5a$. The system is in the metallic state and the density is compressible. (b),(e) The trapping frequency is set by $L = 5.0a$. A MI state is developed at the center. A peak is formed in the entropy distribution $\epsilon(r)$ at the edge of the MI phase because the strong anticorrelation of the MI leads to a reduction of local entropy. (c),(f) The trapping frequency is set by $L = 3.0a$. A band insulator is formed at the center and a ring of the MI exists near $r = 20a$. A metallic state exists elsewhere.

particles are added, but the MI plateau remains for a very large range of particle-number ratios.

This reconfiguration of both fermions is the result of the strong anticorrelation due to their interactions. If there was no interaction, the light fermions would still form a band insulator when heavy fermions are added. The added heavy fermion will form a separate Fermi gas with either a compressible or incompressible state, depending on the trapping potential and particle number. Since there is a tendency at low temperature for the two species to phase separate in a homogeneous mixture [46], the inhomogeneity of the trap and the thermal energy at a finite temperature both act to stabilize this MI phase.

With the SC method, we calculate much larger systems for three-dimensional inhomogeneous systems. We find that the inhomogeneity leads to complex spatial dependence of different phases. In Fig. 3, we show that the radial distributions of the densities, entropy, and double occupancy for a strongly interacting system undergo different phases as the trapping curvature changes. Here, the double occupancy, $d_j = \langle c_j^\dagger c_j f_j^\dagger f_j \rangle$, expresses the probability of having both the light and heavy atom on site j. In Figs. 3(a) and 3(d), we show the case of a shallow potential ($L = 16.5a$). The cloud expands to minimize the kinetic energy and the total density is less than one. The local entropy changes with the density and the double occupancy is almost zero due to the strong repulsive interaction. As the trapping potential becomes strong, the cloud is forced inwards and the density at the

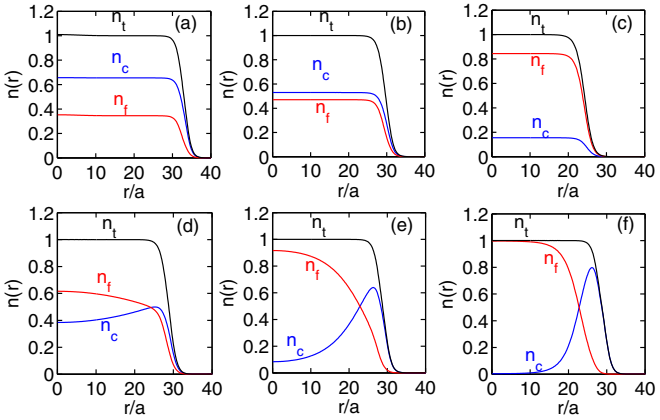

FIG. 4. (Color online) Radial density distribution for systems of asymmetric particle numbers and trap potentials in a 3D system. The interaction is fixed at $U = 50J$ and temperature at $T = 2J/k_B$. (a)–(c) Changing the light particle number, while keeping the heavy particle number fixed at 5×10^4 and trap potentials for both fixed at $L_c = L_f = L = 5a$. The light particle number is (a) 1×10^5, (b) 6×10^4, and (c) 1×10^4. Remarkably, the system remains in a MI phase for all of the range of the particle numbers with the total density fixed at unity, while the individual densities form a plateau at various fractional fillings. (d)–(f) Changing the trap potential of the heavy fermions while keeping the particle number fixed at 5×10^4 for both, and the trap potential for the light fermions fixed at $L_c = 5a$. The trapping potential for the heavy fermions is set by (d) $L_f = 4.9a$, (e) $L_f = 4.5a$, and (f) $L_f = 4a$.

center of the trap increases. When the total density reaches unit filling, the Hubbard band gap prevents it from increasing its density further and a plateau of unit filling is formed. In this region, the cloud size stays largely unchanged as the trap curvature increases. In Figs. 3(b) and 3(e), we show the case of an incompressible MI phase at the center of the trap. It is important to note that in this MI phase, the incompressibility only applies to the total density and the individual densities can still be compressible, which is further demonstrated in Fig. 4. The unit filling of the total density is *not* the result of each species forming an incompressible phase at half filling, but the strong anticorrelation between the light and heavy particles that guarantees there is always *either a light or a heavy particle*. This anticorrelation leads to a reduction of the local entropy, which is most noticeable at the edge of the MI plateau. At the edge, there is a MI and metallic state for almost identical densities. However, the entropy in the metallic state is much higher because the light and heavy particles are less correlated. This leads to a peak in the entropy distribution about the edge. In Figs. 3(c) and 3(f), we discuss the case where the trapping potential is strong enough to force the particle to fill in the upper Hubbard band and a band insulator is formed for both species at the center of trap. Away from the center, there is a secondary plateau that corresponds to the MI phase. In Fig. 3(f), we show distinct behavior of the entropy and double occupancy for different phases. From the center of the trap, the band-insulator state is characterized by a sharp increase of the double occupancy to one and a sharp decrease of the entropy to zero. The metallic state is characterized by an increase of the local entropy. The MI state is characterized by a plateau of the local entropy which is reduced from the entropy of the surrounding metallic state. The double occupancy in both the metallic and the MI state is extremely low as a result of the strong interaction.

The anticorrelation between the particles in the MI phase is further illustrated under asymmetric conditions. First, we consider the case of large particle-number asymmetry. As is shown in Fig. 1 of the MC calculation of the 2D lattice, the MI phase is robust for large number asymmetry. The robustness is confirmed in the SC calculation for 3D systems. We change the light particle number from 1×10^4 to 1×10^5. Remarkably, the system *always* self-organizes into the MI phase, even under extreme particle-number asymmetry. In Figs. 4(a)–4(c), we show the radial density distribution for the cases of $N_c = 1 \times 10^5$, 6×10^4, and 1×10^4. In all three cases, a MI plateau is present at the center of the trap. The plateau is signaled by unit filling of the total density. The radius of the plateau is different in each case because the total particle number is different. For $N_c = 1 \times 10^5$, the individual density forms a plateau at $n_c \approx 0.65$ and $n_f \approx 0.35$. For $N_c = 6 \times 10^5$, the individual density forms a plateau at $n_c \approx 0.55$ and $n_f \approx 0.45$. For $N_c = 1 \times 10^4$, the individual density forms a plateau at $n_c \approx 0.15$ and $n_f \approx 0.85$. The same behavior is observed when we fix the light particle number while changing the heavy particle number. The remarkable robustness of such MI phases also points to a possibility of creating a density plateau at any fractional filling of a species by changing the other species' particle number. We next consider the case of trap frequency asymmetry by varying the trap potential for the heavy particles while keeping the light one fixed via the choice $L_f = 5a$. In the case of asymmetric traps, the difference of the trap potential causes particles to reorganize to minimize their energy. Because the relative density remains compressible, it changes, responding to the difference in the local chemical potential. This is the case for Figs. 4(d) and 4(e). When the difference of the trap potentials is too large, the particles are spatially separated. This is the case in Fig. 4(f), where the center of the trap becomes a band insulator of only heavy particles and the light particles are forced outside the band insulator. Note that this phase separation is different from the phase separation at much lower temperature, which happens for symmetric traps and particle numbers [11]. This phase separation is induced by the asymmetry of the trap potential.

B. Experimental detection

In experiment, the MI phase can be detected from both the mixture's cloud size and the double occupancy following procedures similar to previous experiments with a single species of atoms [1,38]. In addition, the *in situ* radial density profiles discussed previously can also be measured either through selecting a specific 2D plane using a magnetic resonance imaging approach [47] or through the inverse Abel transforms [48,49]. The cloud size of the mixture is determined based on the total radial density profile as

$$R_t = \sqrt{(N_c + N_f)^{-1} \sum_j r_j^2 n_t(r_j)}. \qquad (21)$$

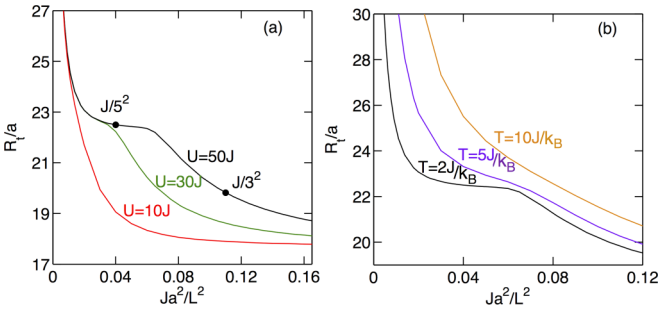

FIG. 5. (Color online) Cloud size R_t of Eq. (21) as a function of the trapping frequency for (a) different interaction U and (b) different temperatures T. The trapping frequencies $\omega_{c\,\mathrm{or}\,f}$ for light and heavy fermions are $\sqrt{2Ja^2/(M_{c\,\mathrm{or}\,f}L^2)}$. The particle number of each species is fixed at 5×10^4. (a) Temperature is fixed at $2J$, and U changes from $10J$ to $50J$. The black dots correspond to the MI and band insulator cases in Fig. 3. (b) Interaction U is fixed at $50J$ and temperature varies from $2J/k_B$ to $10J/k_B$.

Figure 5 shows the cloud size as a function of the trapping frequency for different interaction strengths and different temperatures for a system of 5×10^4 light and heavy particles. In Fig. 5(a), we consider the dependence of the MI phase on the interaction strengths at a given temperature $T=2J/k_B$. When the interaction is relatively small ($U=10J$), the cloud size decreases as the trap potential increases until a band insulator is formed at the center. When the interaction is large ($U=30J$,$50J$), there exists a plateau in the cloud size that corresponds to the MI phase formed at the center of the trap. The plateau appears around $U=30J$ and grows for stronger interactions. In Fig. 5(b), we consider the MI phase at different temperatures with $U=50J$. We find that the critical temperature is around $T=5J$. Above $T=5J$, the cloud size decreases smoothly with an increase of the trap potential. When $T<5J$, the decrease is slowed down and corresponds to the MI phase. For $T=2J/k_B$, a plateau is clearly present.

Due to the repulsive interaction, the double occupancy remains very small for low densities and in the MI phase. Without the existence of the Hubbard band, the double occupancy began to change gradually as the total particle number increases and the density at the center of the trap increases. The effect of the Hubbard band or the MI phase is to suppress the double occupancy and the change of the double occupancy becomes more abrupt as the density at the center of the trap starts to fill in the upper Hubbard band, rather than the gradual increase when the MI is not present. This abrupt change of the double occupancy is captured in the double-occupancy rate, $\partial D/\partial N$. The double occupancy reaches one where the two individual band insulators are formed. In Figs. 6(a) and 6(b), we show our calculation of the average double occupancy as a function of the particle number with a fixed trapping potential and for various interaction strengths. In the case of small interaction ($U=10J$), under the same trap potential, the increase of the particle number increases the density of the cloud and the double occupancy increases smoothly as the individual density increases to unity. As the interaction increases further ($U>30J$), the density increase is suppressed when the MI begins to develop at the center of the trap. This suppression leads to more than an order of magnitude difference in the average double occupancy for systems where a MI plateau is developed. In Fig. 6(c), we show the double-occupancy rate with regard to the particle number as a function of the interaction. The derivative reduces to almost zero at around $U=30J$. It signals that a MI plateau is formed for $U>30J$.

It is worth noting that the critical interaction and temperature indicated in our calculation of a trapped system is not quantitatively the same as those calculated for a homogeneous system. This is because in the trapped system, the Hubbard gap needs to be compared with the potential-energy gradient of the trap. If the gap is so small that the energy difference between neighboring sites at the center of the trap and the thermal fluctuations is sufficient to overcome the gap, a MI plateau will not form. Hence, the measurement of macroscopic quantities, such as the cloud size and average double-occupancy rate, is more appropriate to detect the existence of a collective MI region in the trapped system, instead of a measuring of the critical interaction strength for the corresponding homogeneous system.

C. Comparison with quantum Monte Carlo calculation

Based on the SC calculations, we use the MC method to verify our findings. One of the main advantages of the MC

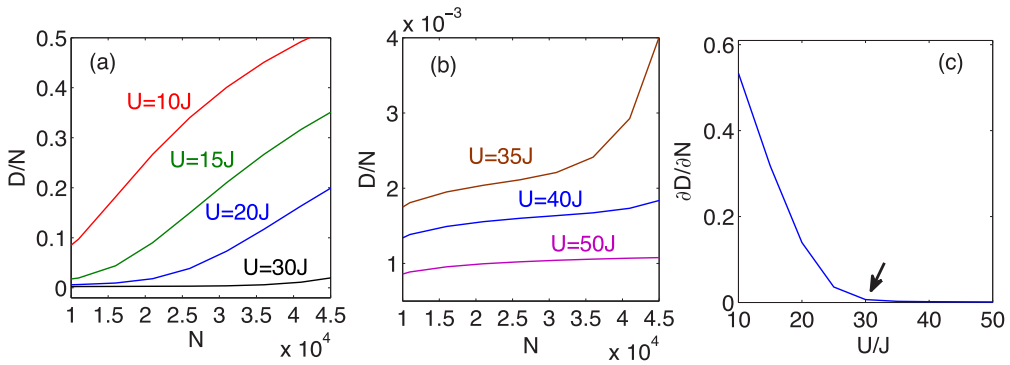

FIG. 6. (Color online) (a),(b) Average double occupancy as a function of the interaction for different temperature. (c) Double-occupancy rate as a function of the interaction. The interaction is fixed at $50J$, the trapping frequency is $J/25$, and the particle number for both species is N. The MI phase occurs at around $U=30J$ when $\partial D/\partial N$ reduces to zero (black arrow).

method is that it operates in real space and therefore it can show not only average density distributions, but also particular configurations of the light and heavy fermions. This is useful to distinguish between disordered phases and phase separation. It also allows us to calculate the density-density correlation functions. From the snapshots of the configurations of the light and heavy fermions, it is easy to calculate the correlation function and demonstrate that the distributions of the light and fermions are strongly anticorrelated, i.e., there are no light fermions on sites occupied by heavy fermions, and vice versa. This, however, does not directly determine the total density, which in the case of the MI should be equal to one. Therefore, in Fig. 2, we show the total density, where the plateau with unit total filling is clearly visible in the center of the system.

This modified MC method allows us to study much larger systems than the fully quantum MC methods. Nevertheless, since in each MC step the Hamiltonian has to be diagonalized, it is much more resource demanding than the traditional MC method for purely classical systems. Moreover, the calculation of the free energy requires the full spectrum of the Hamiltonian

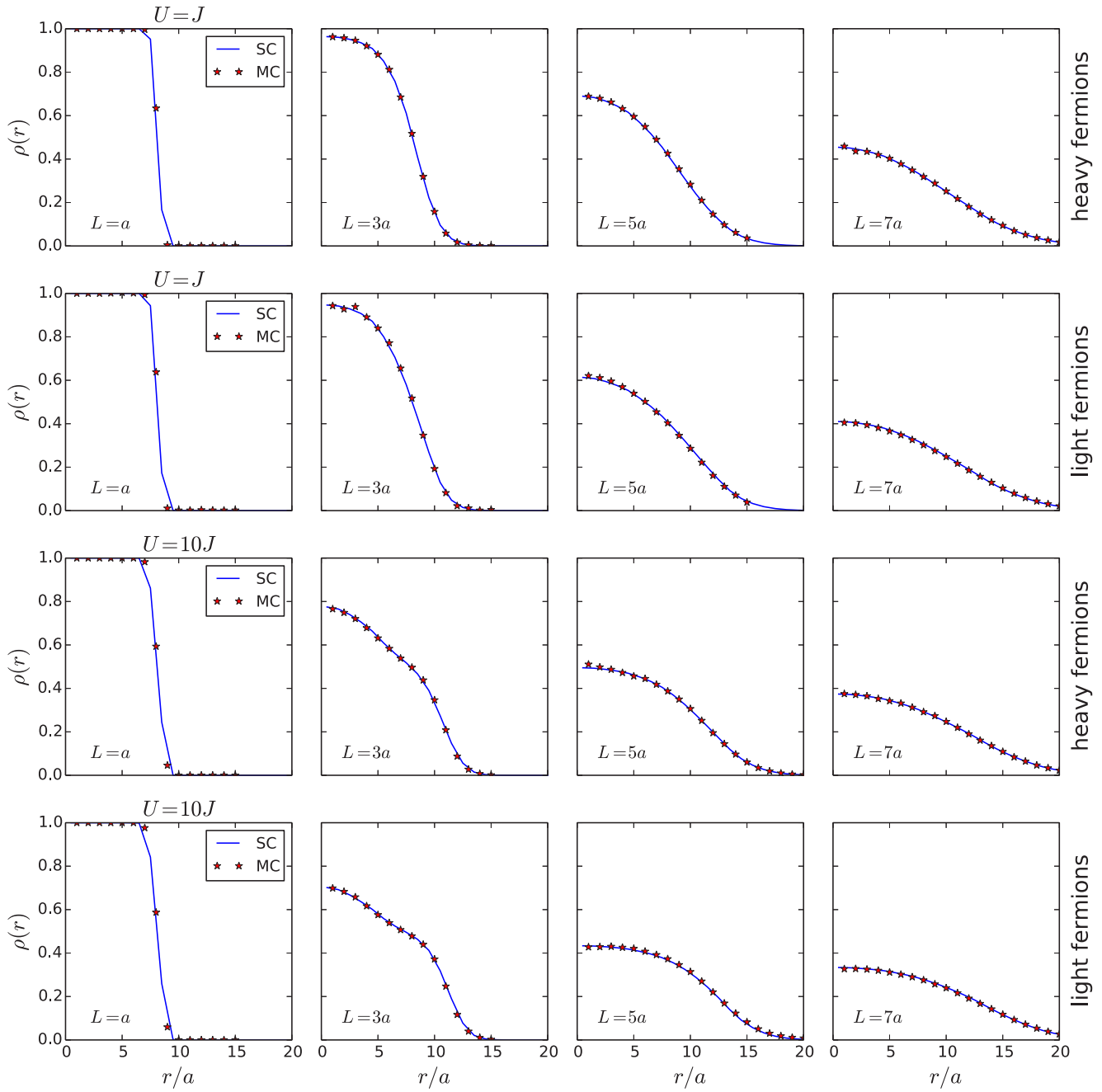

FIG. 7. (Color online) Comparison of the MC (red stars) and SC (blue line) density profiles $\rho(r)$ of the light and heavy fermions calculated for $U = 1J$ and $U = 10J$ for different trap frequencies. The trapping frequency for light and heavy fermions are the same, $L_f = L_c = L$. The system is a 51×51 square lattice with 200 light and 200 heavy fermions. Columns 1 to 4 correspond, respectively, to $L = 1a$, $3a$, $5a$, and $7a$; rows 1 and 3 present profiles of the heavy fermions, whereas rows 2 and 4 present profiles of the light fermions. The interaction U is equal to J in rows 1 and 2 and to $10J$ in rows 3 and 4. The temperature is $2J$.

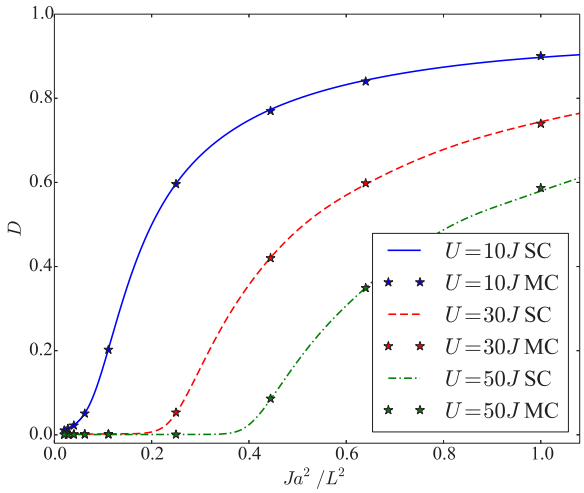

FIG. 8. (Color online) Comparison of the MC (stars) and SC (lines) double-occupancy values as functions of the trap frequency for $U = 10J, 30J, 50J$ in the same lattice system as in Fig. 7.

and therefore selective sparse matrix diagonalization methods such as the Lanczös method cannot be used. As a result, the maximum number of fermions is limited to a few hundred, which is much less than the number of atoms used in real experiments. Therefore, we use the MC approach mainly to show the validity of the SC calculations in the regime of the DMI phase. Since the MI transition is expected for rather strong interaction at temperatures much larger than the ordering temperature, we expect that SC calculations to give accurate results. The comparison with the MC results confirms this assumption. In Fig. 7, we present density profiles calculated with the help of both of the methods and one can see there that even for relatively weak interaction $U = J$, there is no difference between these two approaches.

Since the cloud size is directly related to the density profiles, this comparison guarantees also that the trap-curvature dependence of the cloud radius will be the same in both approaches. We also compared the other parameter that is used to determine the Mott transition, i.e., the number of doubly occupied sites D. Also in this case, we can observe that the dependence of the double occupancy on the trap curvature calculated in the SC approach is the same as that found in the MC calculations. The comparison is presented in Fig. 8.

IV. SUMMARY

In summary, we have demonstrated that despite the fragility of the magnetic or charge density wave ordering in mixtures of atoms with large mass differences, the Mott phase exists at a relative high temperature and in a parameter region that is quite achievable in realistic experimental settings. This phase has demonstrated remarkable robustness against asymmetries, particularly large number imbalance. It points to different ways of realizing novel incompressible densities at fractional fillings with complementary fillings between the species of atoms as the result of strong anticorrelation. Our calculation also shows several possible measurements to detect the MI phase. These calculations are based on previous experiments on MI phases and we considered system sizes comparable to realistic experimental systems. In addition to the Fermi mixtures, similar MI phases can exist for mixtures of heavy-light Bose-Fermi and Bose-Bose atoms in the region where the intraspecies bosonic interaction is stronger than the interspecies interaction.

ACKNOWLEDGMENTS

J.K.F. was supported by a MURI grant from the Air Force Office of Scientific Research (Grant No. FA9559-09-1-0617) and by the McDevitt bequest at Georgetown University. M.M.M. acknowledges support by the Polish National Science Center (NCN) under Grant No. DEC-2013/11/B/ST3/00824. This work was supported by the National Science Foundation under Physics Frontier Center Grant No. PHY-0822671.

[1] R. Jördens, N. Strohmaier, K. Günter, H. Moritz, and T. Esslinger, Nature (London) **455**, 204 (2008).
[2] S. Trotzky, P. Cheinet, S. Fölling, M. Feld, U. Schnorrberger, A. M. Rey, A. Polkovnikov, E. Demler, M. Lukin, and I. Bloch, Science **319**, 295 (2008).
[3] S. Giorgini, L. P. Pitaevskii, and S. Stringari, Rev. Mod. Phys. **80**, 1215 (2008).
[4] G.-B. Jo, Y.-R. Lee, J.-H. Choi, C. A. Christensen, T. H. Kim, J. H. Thywissen, D. E. Pritchard, and W. Ketterle, Science **325**, 1521 (2009).
[5] Y.-A. Liao, A. S. C. Rittner, T. Paprotta, W. Li, G. B. Partridge, R. G. Hulet, S. K. Baur, and E. J. Mueller, Nature (London) **467**, 567 (2010).
[6] D. Greif, T. Uehlinger, G. Jotzu, L. Tarruell, and T. Esslinger, Science **340**, 1307 (2013).
[7] H. Hara, Y. Takasu, Y. Yamaoka, J. M. Doyle, and Y. Takahashi, Phys. Rev. Lett. **106**, 205304 (2011).
[8] C. Kohstall, M. Zaccanti, M. Jag, A. Trenkwalder, P. Massignan, G. M. Bruun, F. Schreck, and R. Grimm, Nature (London) **485**, 615 (2012).
[9] M. Jag, M. Zaccanti, M. Cetina, R. S. Lous, F. Schreck, R. Grimm, D. S. Petrov, and J. Levinsen, Phys. Rev. Lett. **112**, 075302 (2014).
[10] R. A. Duine and A. H. MacDonald, Phys. Rev. Lett. **95**, 230403 (2005).
[11] M. M. Maśka, R. Lemański, J. K. Freericks, and C. J. Williams, Phys. Rev. Lett. **101**, 060404 (2008).
[12] G. J. Conduit, A. G. Green, and B. D. Simons, Phys. Rev. Lett. **103**, 207201 (2009).
[13] G. J. Conduit and B. D. Simons, Phys. Rev. A **79**, 053606 (2009).
[14] S. Pilati, G. Bertaina, S. Giorgini, and M. Troyer, Phys. Rev. Lett. **105**, 030405 (2010).
[15] L. J. LeBlanc, J. H. Thywissen, A. A. Burkov, and A. Paramekanti, Phys. Rev. A **80**, 013607 (2009).
[16] S.-Y. Chang, M. Randeria, and N. Trivedi, Proc. Natl. Acad. Sci. USA **108**, 51 (2011).
[17] X. Cui and T.-L. Ho, Phys. Rev. Lett. **110**, 165302 (2013).
[18] U. Brandt, J. Low Temp. Phys. **84**, 477 (1991).
[19] R. Lemański, J. K. Freericks, and G. Banach, Phys. Rev. Lett. **89**, 196403 (2002).

[20] J. K. Freericks, E. H. Lieb, and D. Ueltschi, Phys. Rev. Lett. **88**, 106401 (2002).
[21] J. K. Freericks, C. Gruber, and N. Macris, Phys. Rev. B **53**, 16189 (1996).
[22] J. K. Freericks, C. Gruber, and N. Macris, Phys. Rev. B **60**, 1617 (1999).
[23] J. K. Freericks and V. Zlatić, Rev. Mod. Phys. **75**, 1333 (2003).
[24] I. Titvinidze, M. Snoek, and W. Hofstetter, Phys. Rev. Lett. **100**, 100401 (2008).
[25] F. Hébert, G. G. Batrouni, X. Roy, and V. G. Rousseau, Phys. Rev. B **78**, 184505 (2008).
[26] I. Titvinidze, M. Snoek, and W. Hofstetter, Phys. Rev. B **79**, 144506 (2009).
[27] T. Keilmann, I. Cirac, and T. Roscilde, Phys. Rev. Lett. **102**, 255304 (2009).
[28] P. P. Orth, D. L. Bergman, and K. Le Hur, Phys. Rev. A **80**, 023624 (2009).
[29] T. S. Mysakovych, J. Phys. Condens. Matter **22**, 355601 (2010).
[30] L. Radzihovsky, Physica C **481**, 189 (2012).
[31] A. B. Kuklov and B. V. Svistunov, Phys. Rev. Lett. **90**, 100401 (2003).
[32] A. Hu, L. Mathey, I. Danshita, E. Tiesinga, C. J. Williams, and C. W. Clark, Phys. Rev. A **80**, 023619 (2009).
[33] M. Iskin, Phys. Rev. A **82**, 033630 (2010).
[34] T. Ohgoe and N. Kawashima, Phys. Rev. A **83**, 023622 (2011).
[35] A. Hu, L. Mathey, E. Tiesinga, I. Danshita, C. J. Williams, and C. W. Clark, Phys. Rev. A **84**, 041609 (2011).
[36] I. Danshita and L. Mathey, Phys. Rev. A **87**, 021603 (2013).
[37] P. G. J. van Dongen and C. Leinung, Ann. Phys. (Berlin) **509**, 45 (1997).
[38] U. Schneider, L. Hackermüller, S. Will, T. Best, I. Bloch, T. Costi, R. Helmes, D. Rasch, and A. Rosch, Science **322**, 1520 (2008).
[39] K. Günter, T. Stöferle, H. Moritz, M. Köhl, and T. Esslinger, Phys. Rev. Lett. **96**, 180402 (2006).
[40] S. Ospelkaus, C. Ospelkaus, O. Wille, M. Succo, P. Ernst, K. Sengstock, and K. Bongs, Phys. Rev. Lett. **96**, 180403 (2006).
[41] T. Best, S. Will, U. Schneider, L. Hackermüller, D. van Oosten, I. Bloch, and D.-S. Lühmann, Phys. Rev. Lett. **102**, 030408 (2009).
[42] S. Sugawa, K. Inaba, S. Taie, R. Yamazaki, M. Yamashita, and Y. Takahashi, Nat. Phys. **7**, 642 (2011).
[43] C. Ates and K. Ziegler, Phys. Rev. A **71**, 063610 (2005).
[44] D. Ueltschi, J. Stat. Phys. **116**, 681 (2004).
[45] M. M. Maśka and K. Czajka, Phys. Rev. B **74**, 035109 (2006).
[46] J. K. Freericks, E. H. Lieb, and D. Ueltschi, Commun. Math. Phys. **227**, 243 (2002).
[47] K. Jiménez-García, R. L. Compton, Y.-J. Lin, W. D. Phillips, J. V. Porto, and I. B. Spielman, Phys. Rev. Lett. **105**, 110401 (2010).
[48] Y. Shin, M. W. Zwierlein, C. H. Schunck, A. Schirotzek, and W. Ketterle, Phys. Rev. Lett. **97**, 030401 (2006).
[49] Y.-i. Shin, C. H. Schunck, A. Schirotzek, and W. Ketterle, Nature (London) **451**, 689 (2008).